The EMBO Journal vol.9 no.1 pp.17 - 24, 1990

The structure of a membrane fusion mutant of the influenza virus haemagglutinin

W.I.Weis[2], S.C.Cusack[3], J.H.Brown, R.S.Daniels[1], J.J.Skehel[1] and D.C.Wiley[4]

Department of Biochemistry and Molecular Biology, and Howard Hughes Medical Institute, Harvard University, Cambridge, MA 02138, USA and [1]National Institute of Medical Research, Mill Hill, The Ridgeway, London, UK

[2]Present address: Department of Biochemistry and Molecular Biophysics, Columbia University, 630 West 168th Street, New York, NY 10032, USA

[3]Present address: EMBL, c/o I.LL., 156X, 38042, Grenoble, Cedex, France

[4]To whom correspondence should be addressed

Communicated by J.J.Skehel

The haemagglutinin glycoprotein (HA) of influenza virus specifically mediates fusion of the viral and host cell endosomal membranes at the acidic pH of endosomes. The HAs from mutant viruses with raised fusion pH optima contain amino acid substitutions in regions of the HA structure thought to be involved in the fusion process [Daniels *et al.* (1985b) *Cell*, 40, 431–439]. We have determined the neutral pH crystal structure of one such mutant, HA_2 112 Asp → Gly. A water molecule appears to partially replace the aspartate side chain, and no changes are observed in the surrounding structure. It appears that four intra-chain hydrogen bonds that stabilize the location of the N-terminus of HA_2 are lost in the mutant, resulting in a local destabilization that facilitates the extrusion of the N-terminus at higher pH.

Key words: haemagglutinin/influenza virus/mutants/structural analysis

Introduction

Viruses with lipid membranes infect cells by processes involving fusion of viral and cellular membranes. For the majority of enveloped viruses, including influenza, fusion occurs in endocytic vesicles and is specifically induced at the acidic pH of these compartments (White *et al.*, 1983). In the case of influenza, the membrane glycoprotein haemagglutinin (HA) mediates the fusion process (White *et al.*, 1982; Sato *et al.*, 1983; Wharton *et al.*, 1986). The HA is a trimer (Wiley *et al.*, 1977) in which each monomer consists of two disulphide-linked chains, HA_1 and HA_2, formed by post-translational cleavage of a single polypeptide precursor which generates the C-terminus of HA_1 and the N-terminus of HA_2. This cleavage is required for virus infectivity (Klenk *et al.*, 1975; Lazarowitz and Choppin, 1975), and specifically for fusion activity (White *et al.*, 1982). The first 10 amino acids of the N-terminus of HA_2 are apolar, and they form the most highly conserved sequence of residues in the molecule (Skehel and Waterfield, 1975). These and other observations have led to the proposal that the N-terminal region of HA_2 is active in the fusion process (Gething *et al.*, 1978; Richardson *et al.*, 1980; Wiley and Skehel, 1987).

The HA undergoes large conformational changes at the pH of fusion (Skehel *et al.*, 1982) which is typically in the range 5.0–5.5 (Maeda and Ohnishi, 1980; Vaananen and Kaariainen, 1980; White and Helenius, 1980; Huang *et al.*, 1981). The water soluble ectodomain of the HA produced by bromelain digestion of virus, BHA (Brand and Skehel, 1972), takes on properties of hydrophobic proteins after exposure to low pH, including self-aggregation into rosettes and binding to lipids and non-ionic detergents (Skehel *et al.*, 1982; Doms *et al.*, 1985). At the pH of fusion, the HA also becomes susceptible to proteolysis (Skehel *et al.*, 1982; Doms *et al.*, 1985), and for the X:31 strain, BHA can be cleaved with trypsin into a soluble fragment containing residues 28–328 of HA_1, and an aggregating fragment consisting of residues 1–27 of HA_1 and 1–175 of BHA_2 (Skehel *et al.*, 1982). The latter can be solubilized by treatment with thermolysin (Daniels *et al.*, 1985a; Ruigrok *et al.*, 1988), which removes the first 23 residues of HA_2. These data indicate that the N-terminal region of HA_2 is responsible for the hydrophobic character of HA at the pH of fusion, and lead to the interpretation that the acid-induced conformational change of the HA results in exposure of the conserved hydrophobic amino terminus (Skehel *et al.*, 1982). The crystal structure of the neutral conformation of X-31 BHA (Wilson *et al.*, 1981) has shown this region to consist of a series of bends partially buried in the trimer interface, extending from near the molecular 3-fold symmetry axis to the surface of the molecule (Figure 1a and b). The structural changes required for its exposure are not known. Circular dichroism measurements indicate that at low pH, BHA has secondary structure similar to that of the neutral pH conformation (Skehel *et al.*, 1982) and cross-linking, sedimentation, electron microscopy, and fluorescence experiments suggest that the low pH transition involves partial dissociation of the trimer and rearrangements of the subunits (Graves *et al.*, 1983; Nestorowicz *et al.*, 1985; Ruigrok *et al.*, 1986; Ruigrok *et al.*, 1988; Wharton *et al.*, 1988; White and Wilson, 1988).

Influenza mutants that fuse at higher pH than wild-type virus have been selected by growth in the presence of agents that raise the pH of endocytic vesicles (Daniels *et al.*, 1985b; Doms *et al.*, 1986) and with monoclonal antibodies (Daniels *et al.*, 1987). The HAs from these mutants predominantly contain single amino acid substitutions, mostly involving charged residues, which can be grouped into two classes by their location in the BHA crystal structure. The first class contains substitutions that appear to destabilize the location of the N-terminal region of HA_2 in the neutral pH conformation, either by loss or weakening of hydrogen bonds to polar atoms in the region, or by substitution of residues that produce unfavourable packing interactions. The second class of substitutions appears to involve the weakening or

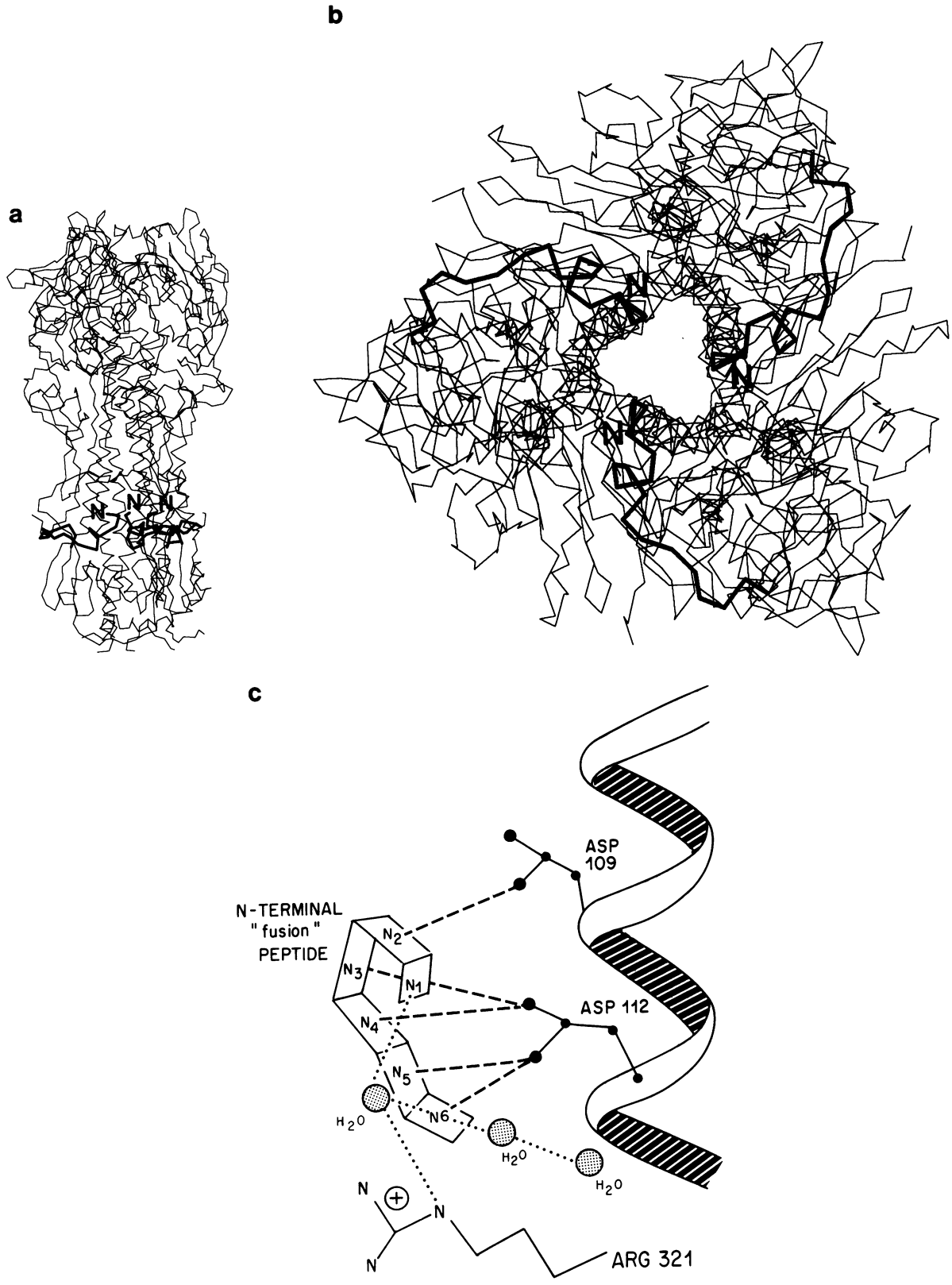

Fig. 1. N-terminal region of HA_2. (a,b) Location of the amino-terminal peptide of HA_2 (thick lines) in the haemagglutinin trimer. The letter 'N' denotes the amino-terminus of HA_2. Only α carbons are shown. (**a**) View with the 3-fold symmetry axis vertical. The viral membrane would be at the bottom of the picture. (**b**) View down the 3-fold symmetry axis, emphasizing the packing of the peptide in the trimer. (**c**) Schematic drawing of the region near HA_2 Asp 112 in the wild-type haemagglutinin. Aspartic acids HA_2 109 and 112 project out from a long helix to form hydrogen bonds (dashed lines) with main chain amide protons on the amino terminal peptide of HA_2. Three ordered water molecules (stippled spheres) lie between arginine 321 of HA_1 and this region, and participate in a linked network of hydrogen bonds indicated by dotted lines. Arg 321 and the water molecules are shown below their actual position for clarity; in this view they would be slightly above and in front of Asp 112 (compare with Figure 3c).

loss of inter-subunit interactions, mostly salt bridges, distant from the N-terminus and throughout the length of the molecule that stabilize the trimer in the neutral pH conformation. The existence of two classes of mutants support the view that both the N-terminus of HA_2 and quartenary structure interactions are involved in the transition. Thermodynamically, the substitutions can be viewed as destabilizing the neutral pH conformation relative to the low pH state, thereby making the low pH induced transition more favourable (Daniels *et al.*, 1985b). The frequency of alterations in charged residues in both classes of mutants indicates their importance in the stabilization of the neutral conformation, and suggests that titration of charged residues may be involved in triggering the conformational change: when enough of these groups are protonated, the stabilizing forces are too weak to maintain the neutral pH conformation, and the transition occurs.

In this report we describe the 3-dimensional structure of

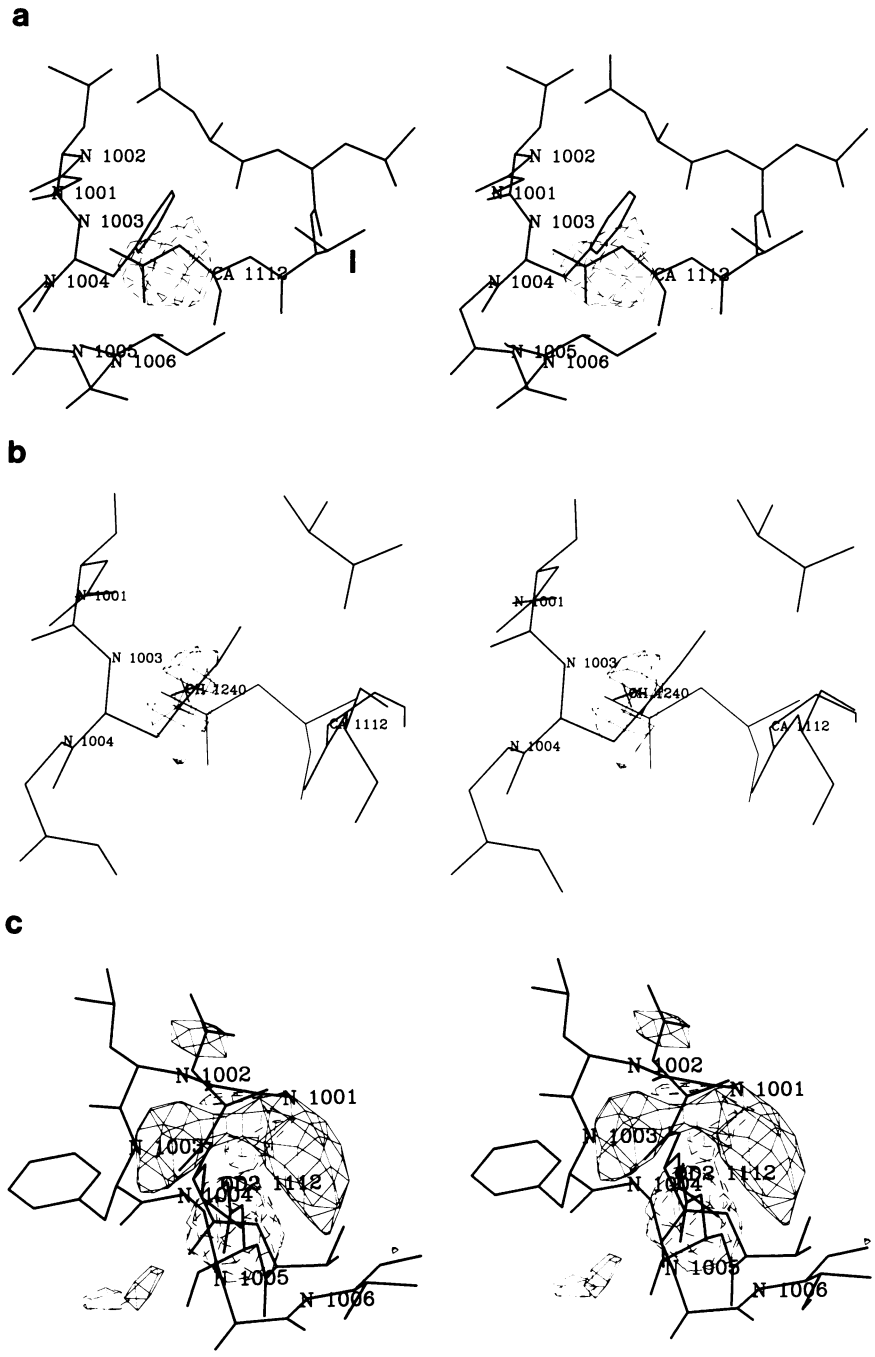

Fig. 2. Difference electron density. (**a**) 3.2 Å difference electron density between the mutant D1112G and wild-type in the HA_2112 region. The map was computed with coefficients $F_o^{[mutant]} - F_o^{[wild\text{-}type]}$ and phases from the refined wild-type model (Weis *et al.*, 1988). The map has been contoured at 6 σ. Negative contours are shown. The refined wild-type coordinates are displayed. (**b**) 3.2 A mutant $F_o - F_c$ map after one round of refinement, showing the position of the water density with respect to the wild-type Asp 1112 side chain. The final refined mutant coordinates are shown, including the water 1240. The wild-type Asp 1112 is shown as thin lines for comparison with the mutant coordinates. The map is contoured at 4 σ. (**c**) Difference electron density map shown in (a), contoured at 4 σ. Positive contours are shown as solid lines, negative as dashed lines. The refined wild-type coordinates are shown. The view is rotated approximately 90° about the vertical from that shown in (a).

the neutral pH conformation of BHA from the single amino acid membrane fusion mutant HA_2 112 Asp→Gly (D1112G) (Daniels *et al.*, 1985b), as determined by X-ray crystallographic difference Fourier analysis. HA_2 112 is located near the bottom of the long helix of HA_2, and forms hydrogen bonds to residues in the amino terminal region of HA_2 (Figure 1c). D1112G therefore falls in the first class of mutants mentioned above, and undergoes the low pH transition 0.4 pH units higher than the wild-type X:31 virus from which it was derived.

Results

The structure of the D1112G mutant HA

The difference electron density between the mutant D1112G and the wild-type (G146D) HAs shows only two strong negative features, i.e., density present in the wild-type that is absent in the mutant. The strongest (13.5 σ), is in the HA_2 112 region (Figure 2a), and clearly shows the absence of the 1112 Asp side chain in the mutant. The other (11.8 σ) lies over the G146D HA_1 Asp 146 side chain, and is due to the known Gly→Asp difference at this position (Knossow *et al.*, 1984), which has no effect on the fusion pH optimum (see Materials and methods). Only one other feature is found over 3.1 σ, and 3.6 σ, and is not near any protein atoms in the crystallographic unit cell.

The difference electron density indicating the loss of the Asp 1112 side chain (Figure 2a) is weak in the vicinity of the wild-type Asp 1112 Oδ2 carboxylate oxygen, and a peak exists at this position in maps calculated with coefficients $2F_o^{[mutant]} - F_o^{[wild\text{-}type]}$ and the same phases (not shown). These results suggest that a water molecule (1240) is present in approximately the same position as the Asp 1112 Oδ2 oxygen in the wild-type molecule, since subtraction of the Asp 1112 Oδ2 density from the water density in the $F_o - F_o$ map leaves no difference density in this region. An $F_o - F_c$ difference map calculated by subtracting amplitudes (F_c) obtained from a model of D1112G after one round of refinement from the observed D1112G amplitudes, F_o, contains a strong peak in the expected position near Oδ2 (Figure 2b). One water molecule (designated 1240) was placed in this position in each of the 3 monomers. Their positions refined stably, and the temperature factors refined to approximately 13 Å^2.

The largest positive difference between the mutant and wild-type electron density (15.8 σ) is a feature that partially surrounds the negative peak on the Asp 1112 side chain (Figure 2c). It does not appear to be due to differences in the structures due to the Asp→Gly change, as no corresponding negative peaks are seen in the map, and no significant differences between the two structures are seen after refinement. The feature is also not in the correct position to be due to the water molecule (1240) that substitutes for the aspartate side chain. Rather, the peak appears to be a Fourier 'ripple' arising from the strong negative density produced by the Asp→Gly difference. (We expect strong difference signals in this region, which is extremely well ordered: the average temperature factor of the Asp 1112 side chain atoms is 4 Å^2, while the average of the molecule is 16 Å^2.) To confirm this interpretation, we computed several model difference electron density ($F_c^{[mutant]} - F_c^{[wild\text{-}type]}$) maps, using calculated structure factors from various mutant models, and the refined wild-type coordinates (not shown). A map using $F_c^{[mutant]}$ calculated from the refined mutant model accurately reproduces the experimental difference map shown in Figure 2a and c. A second map using $F_c^{[mutant]}$ calculated from the refined mutant model, but with the water 1240 removed, has similar features to that shown in Figure 2c, except that the negative contours now contain Oδ2 of the Asp 1112 side chain, and the

Table I. Data processing statistics

Variant	d_{lim} (Å)	$^*R_{int}$	Unique reflections (% of theoretical)	% > 3σ	^+R	r.m.s. deviations from ideality (Å)	
						bond lengths	angle related (1−3) distances
G146D	3.0	0.115	74,765 (83)	71.4	0.209	0.023	0.057
D1112G	3.2	0.160	63,089 (85)	64.7	0.204	0.023	0.058

$$R_{\Delta F} = \frac{\sum_{hkl} ||F_o^{hkl}(D1112G)| - |F_o^{hkl}(G146D)||}{\sum_{hkl} |F_o^{hkl}(D1112G)|} = 0.168$$

$$^*R_{int} \quad \frac{\sum_{hkl}\sum_{obs} |I_{obs}^{hkl} - \langle I^{hkl}\rangle|}{\sum_{hkl}\sum_{obs} I_{obs}^{hkl}}$$

$$^+R = \frac{\sum_{hkl} ||F^{hkl}| - |F_c^{hkl}||}{\sum_{hkl} |F_o^{hkl}|}$$

Data processing statistics are for all reflections between 12 Å and the resolution limit of the data, d_{lim}. Refinement statistics are given for those reflections used in the refinement. For D1112G, all data between 7.0 and 3.6 Å, and reflections for which $|F| \geq 2\sigma(F)$ between 3.6 and 3.2 Å were included in the refinement. For G146D, all data between 7.0 and 3.2 Å, and reflections for which $|F| \geq 2\sigma(F)$ between 3.2 and 3.0 Å were included in the refinement.

positive feature extends farther around the negative peak. This demonstrates that the observed positive difference density is not due to the water molecule (1240) that replaces Asp 1112 Oδ2, although it does show that the water has an effect on the extent of the peak. A third calculated difference map was computed using a 'fake' mutant model made by removing the Asp 1112 side chain atoms from the wild-type model, making no other changes and without adding water 1240. This map looks like the previous map, and shows that the observed positive difference density cannot be due to any small differences in the two structures, Taken together, these results both confirm the correctness of the refined structures and leave a Fourier artefact as the only reasonable interpretation of the positive feature seen in Figure 2c.

In the wild-type HA structure, the Asp 1112 carboxylate oxygens form hydrogen bonds with the amide nitrogens of HA_2 3, 4, 5, and possibly 6 (Table II and Figures 1c and 3c). The loss of this side chain therefore results in the loss of 3 or 4 hydrogen bonds involving a charged acceptor (Asp 1112) which stabilize the position of the N-terminal region of the neutral pH structure. The refined position of the water molecule that replaces the oxygen Oδ2 of the HA_2 112 side chain is such that it does not appear to form the same hydrogen bonds as Asp Oδ2, since it is closer to the α carbons of HA_2 1 and HA_2 112 than to the amide groups of HA_2 3 and HA_2 4. Given the limited resolution of the data and the coordinate error, we cannot exclude the possibility that this water at least partially occupies a more favourable hydrogen bonding position with respect to the HA_2 3 and HA_2 4 main-chain amide groups. Nevertheless, the current coordinates indicate that this water forms a hydrogen bond with another water molecule, as discussed in the following section. A similar result was found recently in a Thr→Gly thermosensitive mutant of phage T4 lysozyme (Alber *et al.*, 1987): a water molecule in the mutant lysozyme structure occupying the same location as the Oγ of a threonine in the wild-type forms the same hydrogen bonds that the threonine makes in the wild-type molecule.

Table II. Potential hydrogen bond distances near HA_2 112

Distances to N-terminal peptide of HA_2 (Å)			
	G146D		D1112G
	Asp 1112 Oδ2	Asp 112 Oδ1	Water 1240
1001 N	3.5		
1003 N	3.0		3.7*
1004 N	2.9		3.7*
1005 N		3.1	
1006 N		3.5	

Distances involving waters 1241–1243 (Å)		
	G146D	D1112G
1241–Gly 1001 N	3.2	3.4
1241–Arg 321 Nε	3.1	2.7
1241–1243	2.7	3.2
1242–Arg 321 N	3.1	3.1
1242–Ile 1108 O	3.1	3.3
1242–Thr 1111 Oγ	3.0	3.2
1242–1243	2.8	2.8
1243–1240 (D1112G only)		3.2

All distances shown are averages of the same distance in the 3 monomers.
Estimated coordinate error (see text) = 0.35 Å.
*Shown only for comparison with Asp 1112 Oδ2.

Structure near HA_2 112

Inspection of difference electron density maps (F_o-F_c) during the refinement process in the HA_2 112 region revealed density that could be accommodated by three water molecules in both the wild-type (Figure 3a) and mutant structures (Figure 3b). This density is also present in $2F_o-F_c$ maps, in difference maps in which the entire surounding area has been deleted from the model, and in the corresponding maps from two other data sets of another X:31 variant, L226Q (Weis *et al.*, 1988). The temperature factors of these water molecules refined to between 12 and 15 $Å^2$ and the refined positions are shown in Figures 3c and d. The three water molecules (designated 1241, 1242 and 1243; Figure 3) apparently form a hydrogen bond-linked network which follows the side chain of Arg 321 of HA_1. At 3 Å resolution, we cannot exclude the possibility that some of the difference density that we have assigned to water is actually N_3^- ion present in the crystallization medium, or, in the case of D1112G, that a citrate ion is present in the region occupied by the four trigonally arranged water molecules (Figure 3d), since there is continuous $2F_o-F_c$ density linking these positions (not shown). We must also consider the possibility that this density represents an alternative conformation of Arg 321. However, the 'water' peak strengths are comparable to the rest of the protein (if these peaks correspond to an alternate conformation of R321, their strength should be proportional to the fractional occupancy of the atoms in this conformation), and no density is seen that would connect R321 Cα to Cγ in the alternate conformation. In the mutant D1112G, the central water of the three, 1243, can also form a hydrogen bond to water 1240 (which substitutes for the Asp 1112 side chain).

Water 1241 bridges the ε-nitrogen of Arg 321 and the amino terminus of HA_2 (Figure 3), which are separated by approximately 6 Å. The angle formed by the amino terminal nitrogen, the water, and Nε 321 is about 150°. It is therefore possible that the density that we have assigned to water 1241 is actually a negatively charged ion such as Cl^-.

Discussion

All influenza mutants with altered pH of fusion found to date have been rationalized in terms of localized effects on the 3-dimensional structure of the neutral pH form of the wild-type HA (Daniels *et al.*, 1985b; Daniels *et al.*, 1987; Doms *et al.*, 1986; reviewed in Wiley and Skehel, 1987): the amino acid substitutions result in the loss of groups that stabilize the structure of the HA_2 N-terminal region or of the trimer interface such that fewer acid-titratable groups must be protonated to disrupt the neutral structure and effect the transition. The difference Fourier analysis presented here demonstrates that the structural effect of the Asp→Gly HA_2 112 change is completely local, with no detectable changes in the surrounding protein structure. It appears that four intra-chain hydrogen bonds which stabilize the location of the N-terminus of HA_2 are lost in the mutant. At 3 Å resolution, the net loss of hydrogen bonds accompanying the apparent substitution of a water molecule for the aspartic acid side chain cannot be determined with

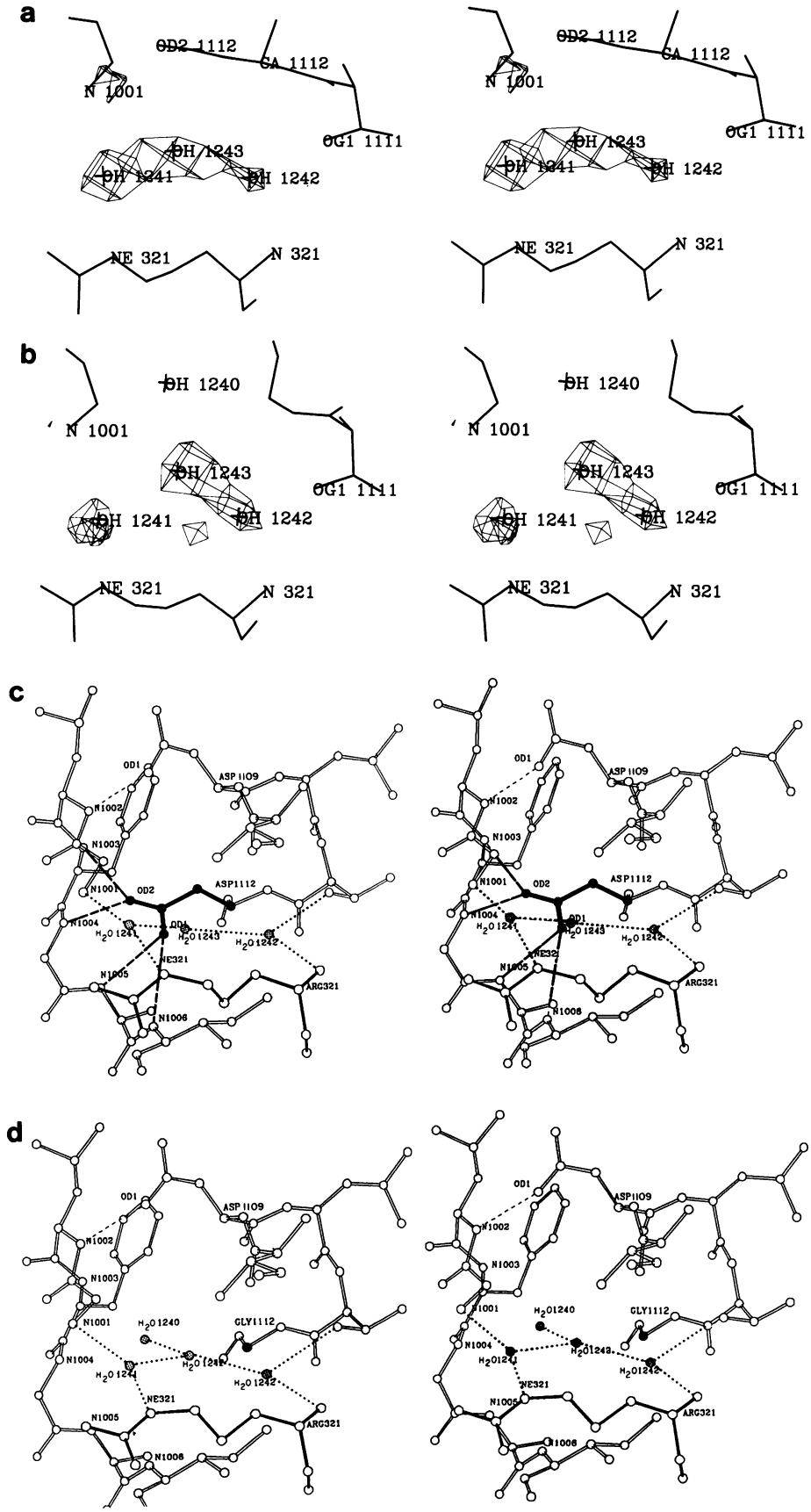

Fig. 3. Water structure near the residue HA_2 112 in the wild-type and mutant HA. **(a)** 3.0 Å F_o-F_c map of the wild-type before waters 1241−1243 were added to the model. The final coordinates are shown, including these waters. The map is contoured at 3 σ.
(b) 3.2 Å F_o-F_c map of mutant D1112G before waters 1241−1243 were added to the model. The final mutant coordinates are shown, including these three waters. The map is contoured at 3 σ. **(c)** Potential hydrogen bond in the 1112 region of the wild-type G146D.
(d) Potential hydrogen bonds in the 1112 region of the mutant D1112G.

certainty. Nevertheless, even if the water (1240) does form hydrogen bonds with N1003 and N1004, there is both a net loss of one or two hydrogen bonds and a decrease in the strength of the remainder resulting from the use of a neutral water molecule as a hydrogen bond acceptor in place of the negatively charged aspartic acid carboxylate oxygens. The loss of hydrogen bonds, as well as the loss of an acid titratable residue that may require protonation as part of the low pH transition, provides a qualitative explanation of the mutant phenotype. We cannot quantitatively relate the loss of stabilization energy due to removal of the aspartate group to the increase in fusion pH optimum, as this would require knowledge of which groups must be protonated to effect the transition, as well as their pK_as, in order to obtain equilibrium constants and hence free energy changes for the transition.

Residue 321 of HA_1 is always a positively charged amino acid: arginine in 43 and lysine in 3 of the 46 known HA_1 sequences from natural influenza isolates. A positive charge near the amino terminus of HA_2 is therefore a conserved feature of the HA structure. No compensating negative charges from protein side chains are in the vicinity of Arg 321, although, since this residue is partially exposed to the surrounding bulk solvent, its charge may be somewhat dispersed. Even with a water molecule or an anion bridging Nϵ 321 to the amino terminus of HA_2, it would appear that this residue destabilizes this region by providing excess positive charge. Circumstantial evidence for such destabilization is provided by the amantadine hydrochloride-selected fusion mutant E1114K, which undergoes the low pH transition 0.6 pH units higher than the parent virus. Glu 1114 forms a salt bridge with Lys 1117 which is only 4.9 Å from the amino terminus of HA_2 of an adjacent monomer (in naturally occurring strains, when 1114 is not glutamic acid, 1117 is not lysine). As discussed previously (Daniels *et al.*, 1985b), the Glu → Lys substitution leaves Lys 1117 as an uncompensated positive charge in the vicinity of the amino terminus of HA_2, and thus destabilizes the neutral pH structure. Based on these observations, we would expect that changing Arg 321 to an uncharged residue would stabilize the neutral pH conformation in this region and thereby lower the pH of fusion. However, the mutant R321Q made by site-directed mutagenesis has a fusion pH similar to that of the wild-type virus (D.Steinhauer *et al.*, unpublished). In the absence of a crystal structure of the R321Q HA, we cannot be certain that this change does not alter some other aspect of the structure. Nonetheless, this result suggests that the species represented by the electron density between Nϵ 321 and the amino terminus of HA_2 may compensate for the excess charge provided by the arginine.

Materials and methods

Nomenclature

The haemagglutinins used in this work are single amino acid variants of the HA from X:31 virus, a recombinant strain containing the HA of the A/Aichi/68 (H3N2) virus. Mutants are named as follows: (single letter code of amino acid in X:31) (residue number) (single letter code of amino acid in mutant), with amino acids numbered 1−328 in HA_1 and 1001−1175 in HA_2. For example, D1112G contains the substitution Asp → Gly at HA_2 112. In this report, 'wild-type' refers to the X:31 antigenic variant G146D, which has a fusion optimum identical to that of X:31. HA_1 146 is approximately 80 Å from HA_2 112, and the X:31 and G146D HAs have identical structures in the HA_2 112 region (Knossow *et al.*, 1984).

Virus and HA purification were as previously described (Skehel *et al.*, 1982).

Crystallization, data collection and refinement

Details of crystalization, film data collection and processing are given in Weis *et al.* (1988), and are summarized in Table I. D1112G was soaked in (2,6)sialyllactose, an influenza receptor analogue, as part of a study of HA-receptor interactions (Weis *et al.*, 1988). The amino acid substitution is approximately 80 Å from the receptor binding site, and it is assumed that receptor binding has no effect on this region, since binding of sialyllactose to the L226Q HA has no effect on the structure in this region (Weis *et al.* 1988). All electron density maps shown have been averaged about the molecular 3-fold symmetry axis, using the programs of Bricogne (1976); however, the same features are found in each monomer on unaveraged maps.

Peak significance was assessed with a program that defines a single peak as a set of contiguous grid points with electron density values above an input threshold. The sum of the density in this set is taken as an estimate of the integrated electron density of the peak. Peaks are ranked according to their number of standard deviations (σ) above the mean density value of all peaks found by the program at a given threshold. This peak definition includes the criterion of strong individual density points, but also considers the presence of a continuous volume of density that corresponds to a real set of atoms. We have found this to be a useful guide in difference Fourier analysis, particularly when difference density arises from many atoms, e.g., when backbone movements occur, as this definition makes no assumption about the shape of the difference density. Moreover, the ranking of strong peaks is relatively insensitive to the input threshold, typically 2 or 3 standard deviations of the map. The peak significances quoted were computed from 3-fold averaged maps, with a 3 standard deviation threshold.

Crystallographic refinement was carried out using the procedure of Hendrickson and Konnert (Hendrickson, 1985). The entire trimeric asymmetric unit was refined, but restraints were applied to maintain appoximate non-crystallographic 3-fold symmetry (Hendrickson, 1985). All interatomic distances reported in this work are averages of the same distance found in each of the 3 monomers. Based on Luzzati analysis (Luzzati, 1952) and r.m.s. deviation of superimposed monomers, we estimate the coordinate error to be approximately 0.35 Å.

Individual isotropic atomic temperature (B) factors were refined. Although the effect of the temperature factors on the scattering factors varies relatively slowly at 3 Å resolution, they do reflect the large variation in order seen in a molecule as large as the HA, which has large portions buried in a well-ordered trimer interface. Water molecules were placed in the model if they met the following criteria. (i) Present in both averaged and unaveraged $F_o - F_c$ maps. (ii) Present in the same positions in isomorphous structures (Weis *et al.*, 1988). (iii) Positions and temperature factors refined stably. (iv) Contour level above significant peaks in bulk solvent region. (v) Reasonable hydrogen bonding geometry.

Acknowledgements

We thank David Stevens for excellent technical assistance. D.C.W. acknowledges support from the NIH AI 13654 and the Howard Hughes Medical Institute. W.W. was supported by NSF and W.R.Grace Co. predoctoral fellowships.

References

Alber,D, Dao-pin,S., Wilson,K., Wozniak,J.A., Cook,S.P. and Matthews,B.W. (1987) *Nature*, **330**, 41−46.

Brand,C.M. and Skehel,J.J. (1972) *Nature (New Biol.)*, **238**, 145−147.

Bricogne,G. (1976) *Acta Crystalogr*, **A32**, 832−847.

Daniels,R.S., Douglas,A.R., Skehel,J.J., Waterfield,M.D., Wilson,I.A. and Wiley,D.C. (1985a) In Laver,W.G. and Chu,CM. (eds), *The Origin of Pandemic Influenza Viruses*. New York: Elsevier-North Holland.

Daniels,R.S., Downie,J.C., Hay,A.J., Knossow,M., Skehel,J.J., Wang,M.L. and Wiley,D.C. (1985b) *Cell*, **40**, 431−439.

Daniels,R.S., Jeffries,S., Yates,P., Schild,G.C., Rogers,G.N., Paulson,J.C., Wharton,S.A., Douglas,A.R., Skehel,J.J. and Wiley,D.C. (1987) *EMBO J.*, **6**, 1459−1465.

Doms,R.W., Helenius,A. and White,J. (1985) *J. Biol. Chem.*, **260**, 2973−2981.

Doms,R.W., Gething,M.-J., Henneberry,J., White,J. and Helenius,A. (1986) *J. Virol.*, **57**, 603−613.

Gething,M.J., White,J. and Waterfield,M.D. (1978) *Proc. Natl. Acad. Sci. USA*, **75**, 2737−2740.

Graves,P.N., Schulman,J.L., Young,J.F. and Palese,P. (1983) *Virology*, **126**, 106−116.

Hendrickson,W.A. (1985) *Methods Enzymol.*, **115**, 252−270.

Huang,R.T.C., Rott,R. and Klenk,H.-D. (1981) *Virology*, **110**, 243–247.
Klenk,H.-D., Rott,R., Orlich,M.F. and Blodorn,J. (1975) *Virology*, **68**, 426–439.
Knossow,M., Daniels,R.S., Douglas,A.R., Skehel,J.J. and Wiley,D.C. (1984) *Nature*, **311**, 678–680.
Lazarowitz,S.G. and Choppin,P.W. (1975) *Virology*, **68**, 440–454.
Luzzati,V. (1952) *Acta Crystalogr.*, **5**, 802–810.
Maeda,T. and Ohnishi,S. (1980) *FEBS Lett.*, **122**, 283–287.
Nestorowicz,A., Laver,W.G. and Jackson,D.C. (1985) *J. Gen. Virol.*, **66**, 1687–1695.
Richardson,C.D., Scheid,A. and Choppin,P.W. (1980) *Virology*, **105**, 205–222.
Ruigrok,R.W.H., Wrigley,N.G., Calder,L.J., Cusack,S., Wharton,S.A., Brown,E.B. and Skehel,J.J. (1986) *EMBO J.*, **5**, 41–49.
Ruigrok,R.W.H., Aitken,A., Calder,L.J., Martin,S.R., Skehel,J.J., Wharton,S.A., Weis,W. and Wiley,D.C. (1988) *J. Gen. Virol.*, **69**, 2785–2795.
Sato,S.B., Kawasaki,K. and Ohnishi,S. (1983) *Proc. Natl. Acad. Sci. USA*, **80**, 3153–3157.
Skehel,J.J. and Waterfield,M.D. (1975) *Proc. Natl. Acad. Sci. USA*, **72**, 93–97.
Skehel,J.J., Bayley,P.M., Brown,E.B., Martin,S.R., Waterfield,M.D., White,J.M., Wilson,I.A. and Wiley,D.C. (1982) *Proc. Natl. Acad. Sci. USA*, **79**, 968–972.
Vaananen,P. and Kaariainen,L. (1980) *J. Gen. Virol.*, **46**, 467–475.
Weis,W., Brown,J.H., Cusack,S., Paulson,J.C., Skehel,J.J. and Wiley,D.C. (1988) *Nature*, **333**, 426–431.
Wharton,S.A., Skehel,J.J. and Wiley,D.C. (1986) *Virology*, **149**, 27–35.
Wharton,S.A., Ruigrok,R.W.H., Martin,S.R., Skehel,J.J., Bayley,P.M., Weis,W. and Wiley,D.C. (1988) *J. Biol. Chem.*, **263**, 4474–4480.
White,J.M. and Helenius,A. (1980) *Proc. Natl. Acad. Sci. USA*, **77**, 3273–3277.
White,J., Helenius,A. and Gething,M.-J. (1982) *Nature*, **300**, 658–659.
White,J., Kielian,M. and Henenius,A. (1983) *Quart. Rev. Biophysics*, **16**, 151–195.
White,J. and Wilson,I. (1988) *J. Cell. Biol.*, **105**, 2887–2896.
Wiley,D.C., Skehel,J.J. and Waterfield,M.D. (1977) *Virology*, **79**, 446–448.
Wiley,D.C. and Skehel,J.J. (1987) *Annu. Rev. Biochem.*, **56**, 365–394.
Wilson,I.A., Skehel,J.J. and Wiley,D.C. (1981) *Nature*, **289**, 366–373.

Received August 25, 1989

Note added in proof

A recently re-refined G146D model (W.I.Weis, A.T.Brünger, J.J.Skehel and D.C.Wiley, *J. Mol. Biol.*, in press) has the N-terminus of HA_2 2.9 Å from HA_2Asp 112 Oδ2 (compare with Table IIa), indicating that a salt bridge may exist between those two groups. None of the qualitative conclusions presented above are affected by this change.